Supplemental Figure Legends

FIGURE S1

A

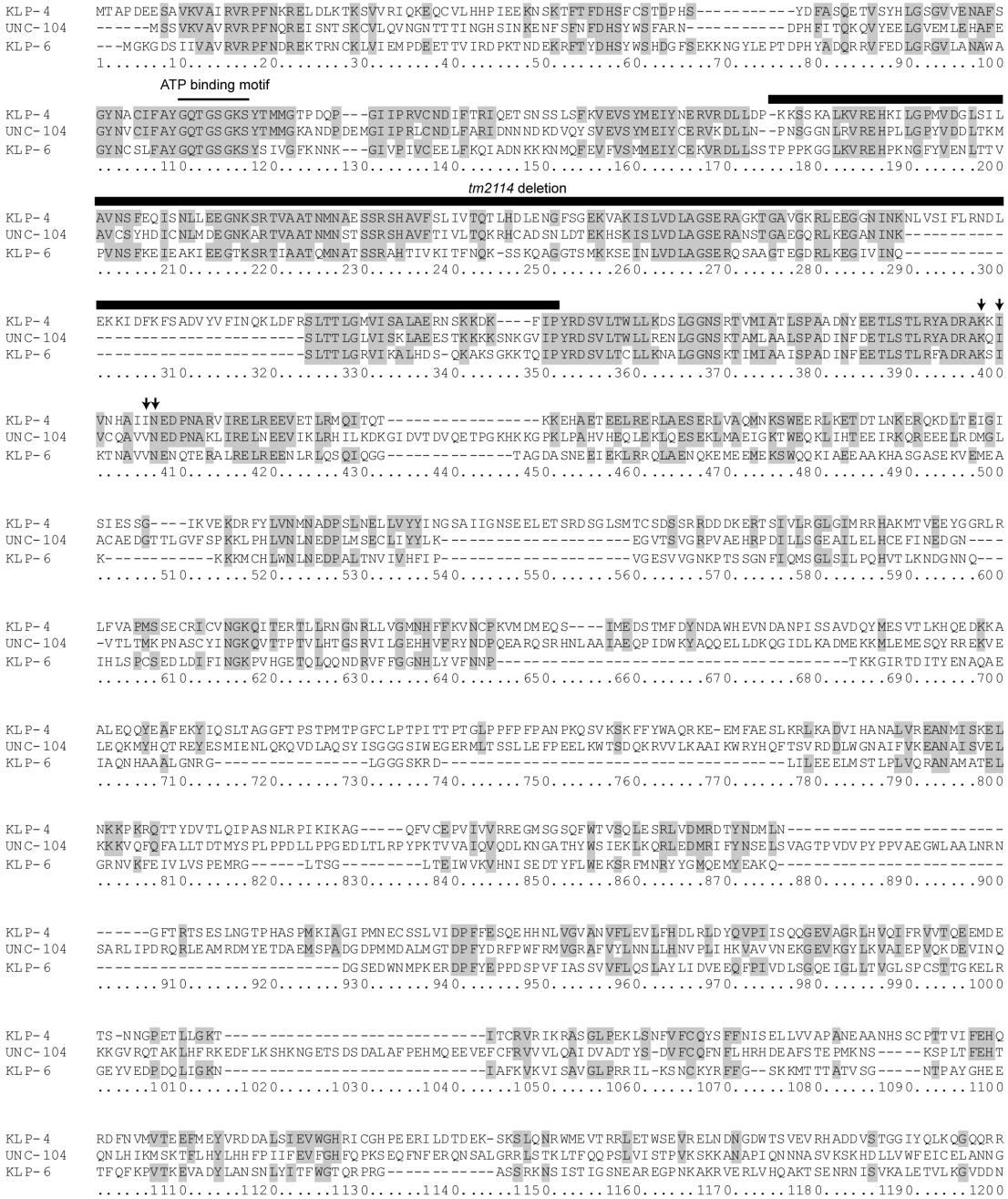

FIGURE S1 (part 2)

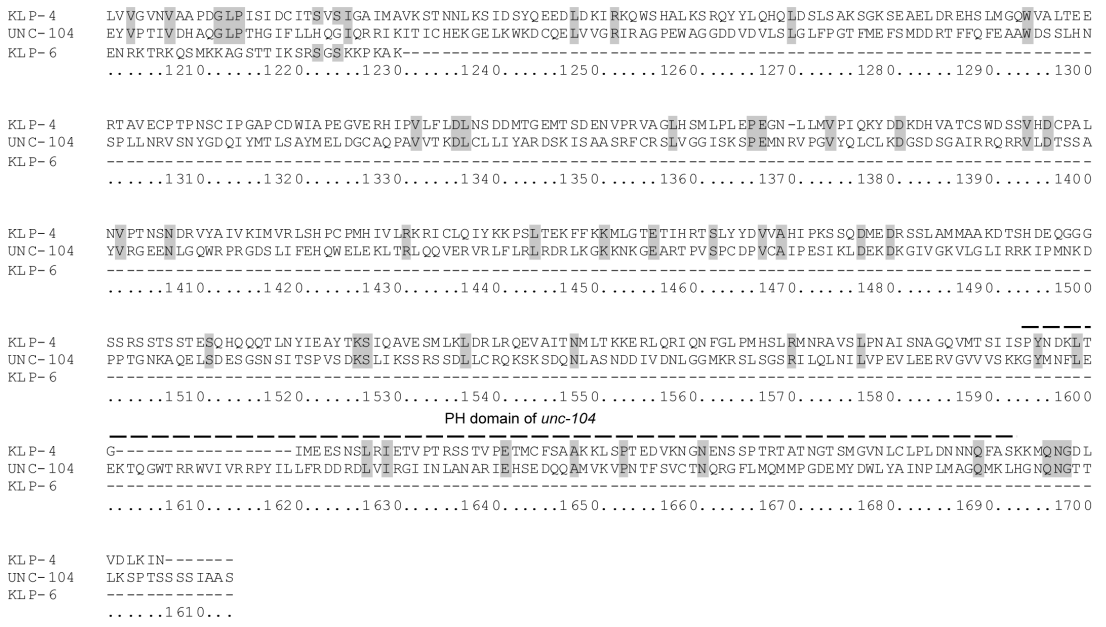

B

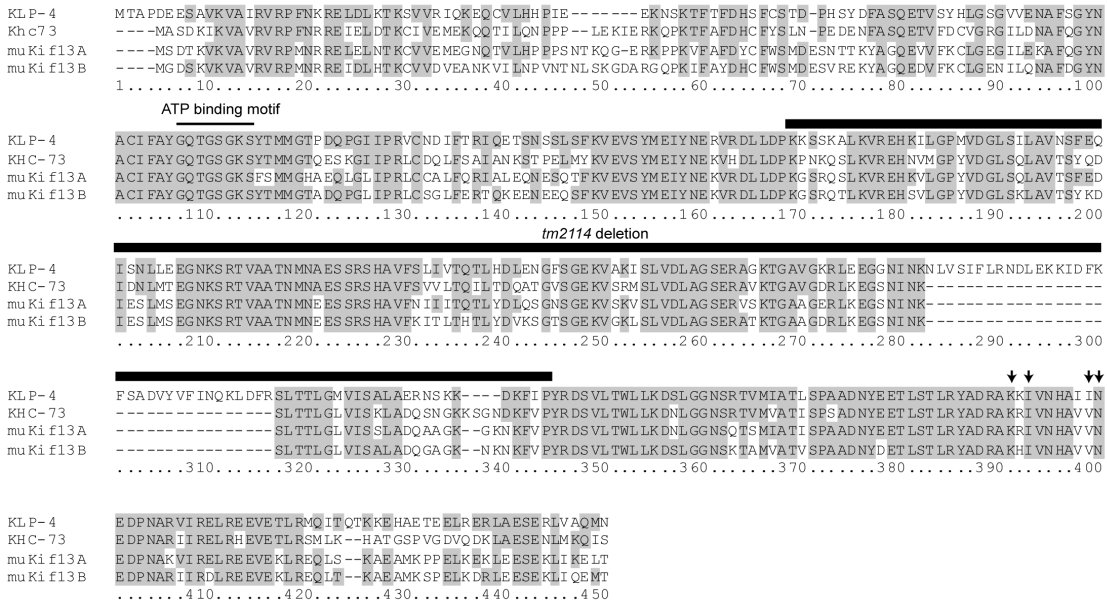

FIGURE S1. Protein alignment of the motor domain of KLP-4 and its homologs.

(A) ClustalW2 multiple sequence alignment of amino acids in *C. elegans* KLP-4, UNC-104 and KLP-6. Identical residues between KLP-4 and the other homologs are boxed

and shaded in grey. The thin black line marks the ATP binding motif. Black arrows mark the conserved residues found in microtubule plus-end directed kinesins. The thick black line demarcates the *tm2114* deletion. The dotted line indicates the location of the PH domain in UNC-104. (B) ClustalW2 multiple sequence alignment of amino acids in the motor domains of *C. elegans* KLP-4, *Drosophila* Khc73, mouse KIF13A and mouse KIF13B. Identical residues between KLP-4 and the other three homologs are boxed and shaded in grey. The thin black line marks the ATP binding motif. Black arrows mark the conserved residues found in microtubule plus-end directed kinesins. The thick black line demarcates the *tm2114* deletion.

FIGURE S2

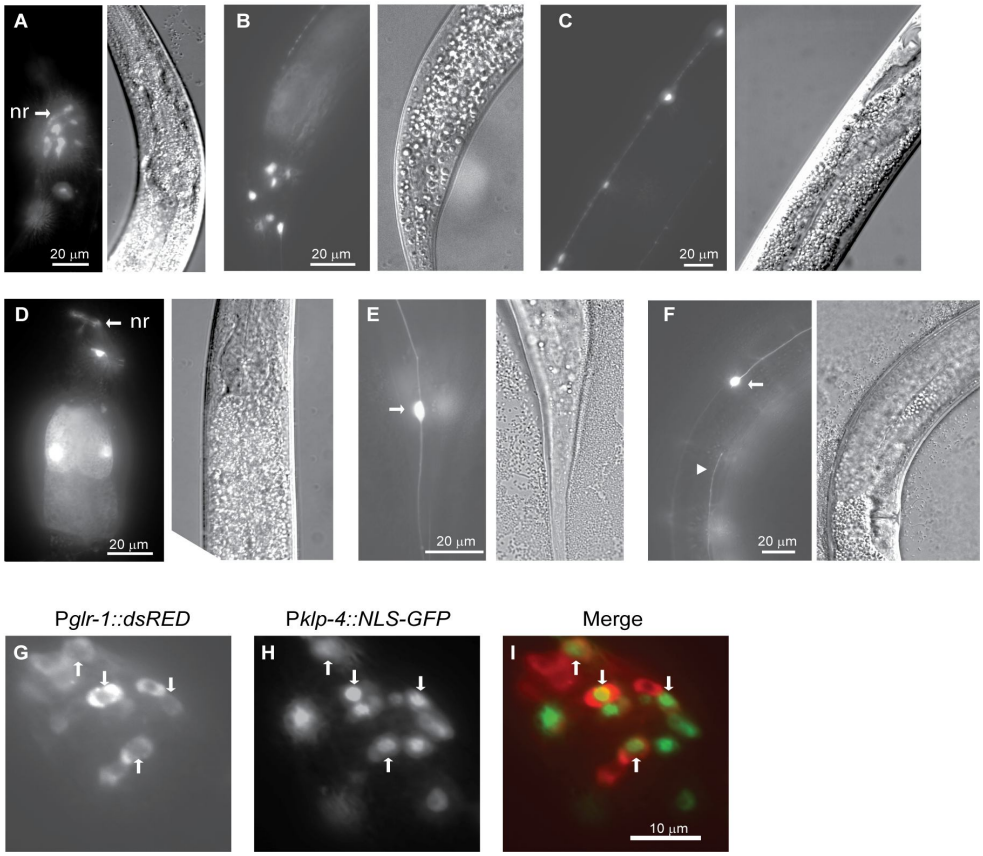

FIGURE S2. KLP-4 is expressed throughout the nervous system and in other tissues. (A-F) Images of animals expressing a *klp-4* transcriptional reporter consisting of GFP under the control of the *klp-4* promoter *(pzEx256)*. GFP signal is shown in neuronal cell bodies of the head (A) and tail (B), and ventral nerve cord (C) as well as in the nerve ring (nr) (A, D) and the mechanosensory neurons PLM (E) and ALM (F) Arrows mark the cell body of PLM in (E) and ALM in (F), respectively. An arrowhead marks the anterior process of PLM in (F). In all images, anterior is oriented towards the top of the image. (G-I) Images of neuronal cell bodies in the head of an animal co-expressing a *glr-1* transcriptional reporter (P*glr-1::dsRED*) (G) and a *klp-4* transcriptional reporter (P*klp-4::NLS::GFP*) (H). (I) Merged image of (G) and (H). Neurons co-expressing *klp-4* and *glr-1* are indicated by the white arrows.

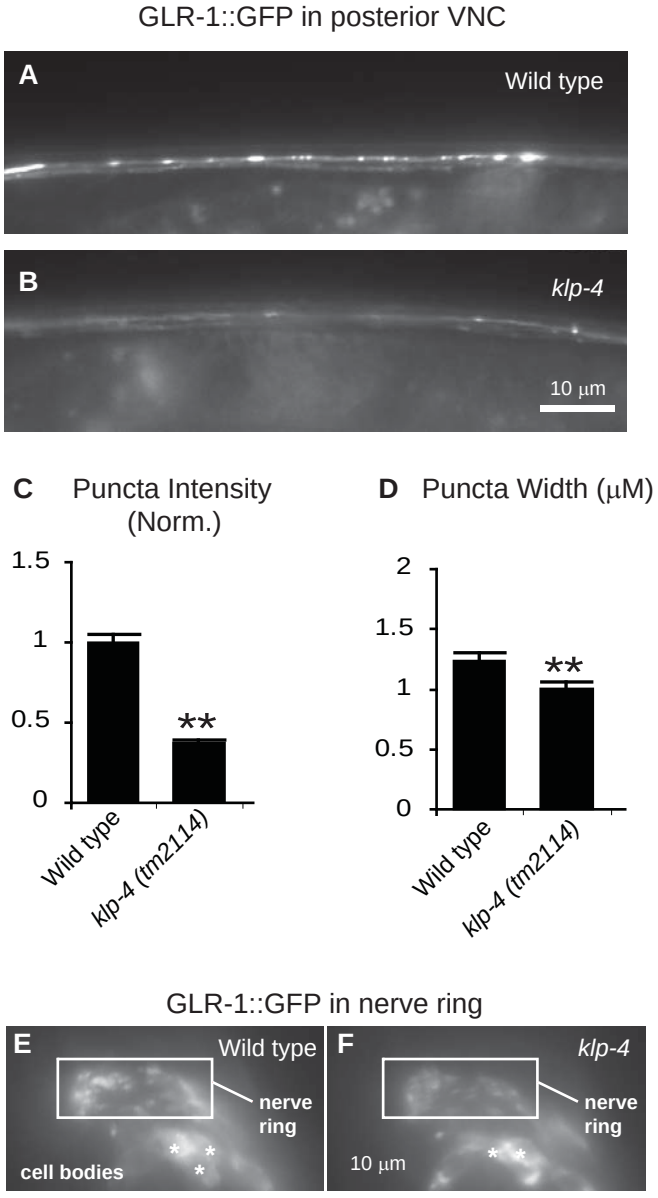

FIGURE S3. KLP-4 promotes the abundance of GLR-1 in the posterior VNC and nerve ring of *C. elegans*. (A-B) Representative images of the posterior VNC (immediately posterior to the vulva) of L4 stage wild-type (A), and *klp-4(tm2114)* (B) animals expressing GLR-1::GFP (*nuIs25*). (C-D) Quantification of GLR-1::GFP puncta intensities (normalized) (C) for the strains pictured in A-B. Means and SEM are shown for *n* = 28 wild type and *n* = 21 *klp-4(tm2114)* animals. Values that differ significantly from wild type are indicated by asterisks above each bar (**p < 0.001, Student's *t*-test). (E-F) Representative images of a section of the nerve ring and adjacent cell bodies of L4 stage wild-type (E) and *klp-4(tm2114)* (F) animals expressing GLR-1::GFP (*nuIs25*). The nerve ring section is demarcated by a white box and cell bodies are marked with white asterisks. Images are oriented with anterior to the top.

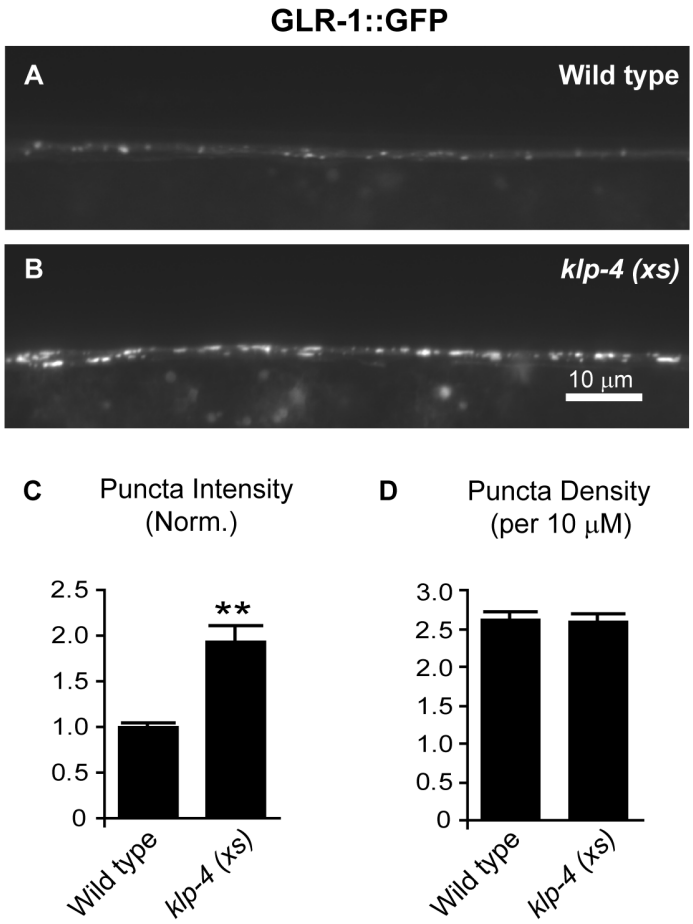

FIGURE S4. KLP-4 overexpression increases GLR-1 abundance in the anterior VNC of *C. elegans*. (A-B) Representative images of GLR-1::GFP *(nuIs25)* in the anterior VNC of L4 stage wild-type (A), and wild-type animals that express *klp-4* cDNA under the control of the *glr-1* promoter [*klp-4(xs)*] (*pzIs20*) (B). (C-D) Quantification of GLR-1::GFP puncta intensities (normalized) (C) and densities (D) for the strains pictured in A-B. Means and SEM are shown for *n* = 15 wild type and *n* = 18 *klp-4(xs)* animals.

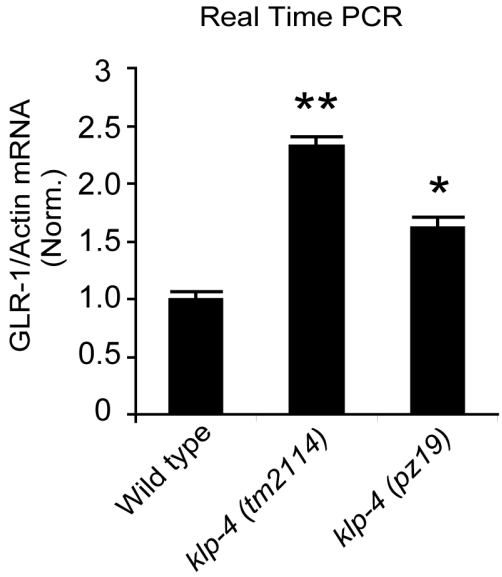

FIGURE S5. Analysis of *glr-1* transcript levels in *klp-4* mutants. Results of real-time quantitative PCR are shown. *glr-1* to *act-1* (actin) mRNA ratios are shown for wild-type, *klp-4(tm2114)* and *klp-4(pz19)* animals expressing GLR-1::GFP *(nuIs25)* (normalized to wild-type). For each genotype, n = 6 replicate measurements of *glr-1* mRNA level were normalized to the average of n = 6 replicate measurements of actin mRNA level. Mean and SEM are shown. Values that differ significantly from wild type are indicated by asterisks above each bar (**$p \leq 0.001$, *$p \leq 0.01$ Student's t-test).

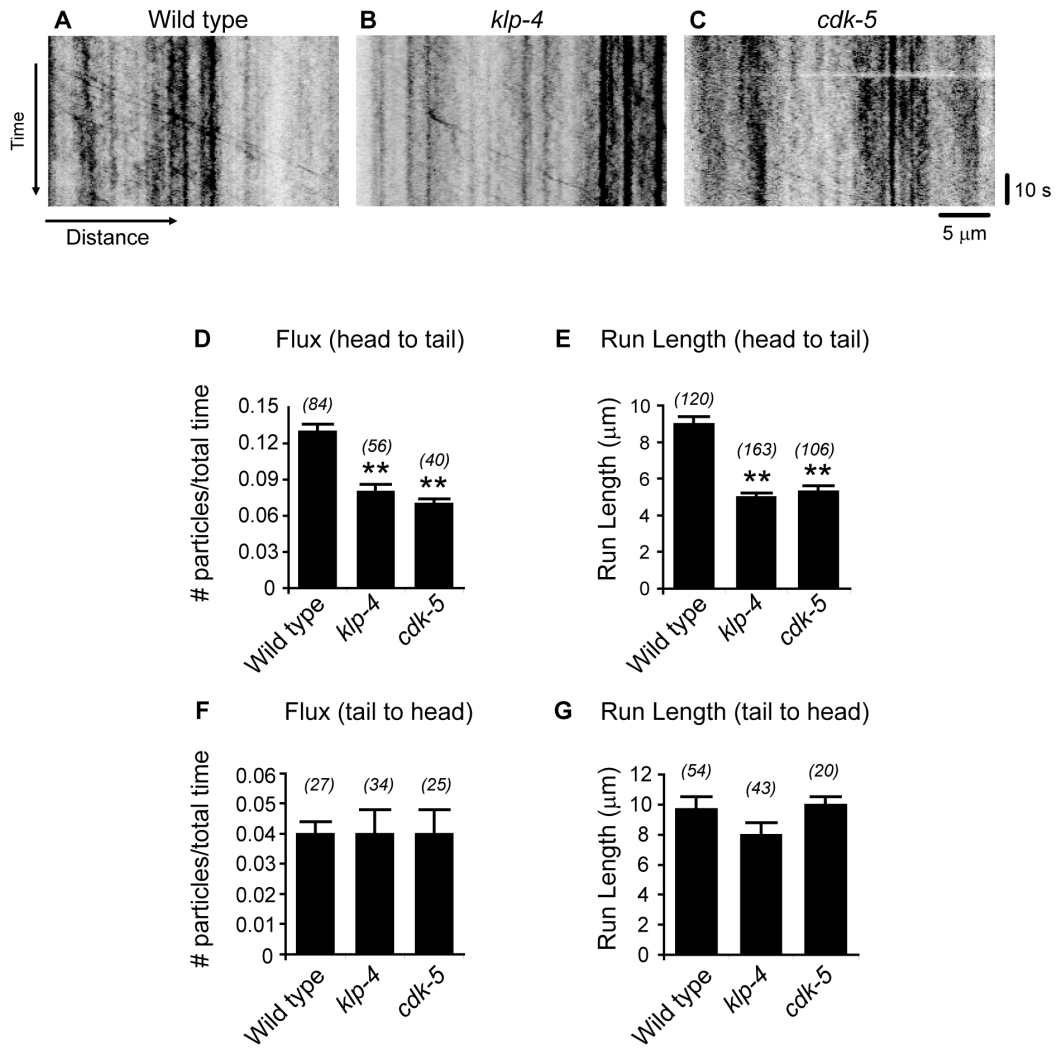

FIGURE S6. KLP-4 and CDK-5 regulate the trafficking of GLR-1::GFP in the VNC. (A-C) Representative kymographs showing mobile and stationary GLR-1::GFP puncta in the anterior VNC of young adult wild type (A), *klp-4(tm2114)* (B) and *cdk-5(gm336)* (C) animals expressing GLR-1::GFP (*nuIs25*). For all kymographs, anterior is to the left. (D-G) Quantification of average flux (D, F), and run length (E, G) for GLR-1::GFP puncta moving towards the tail (D-E) or towards the head (F-G) for wild type, *klp-4* and *cdk-5*. Mean and SEM are shown. The number of events (*n*) analyzed for each parameter is indicated above the bars on the graphs. Values that differ significantly from wild type are indicated by asterisks above each bar (**p<0.001, Student's t test).

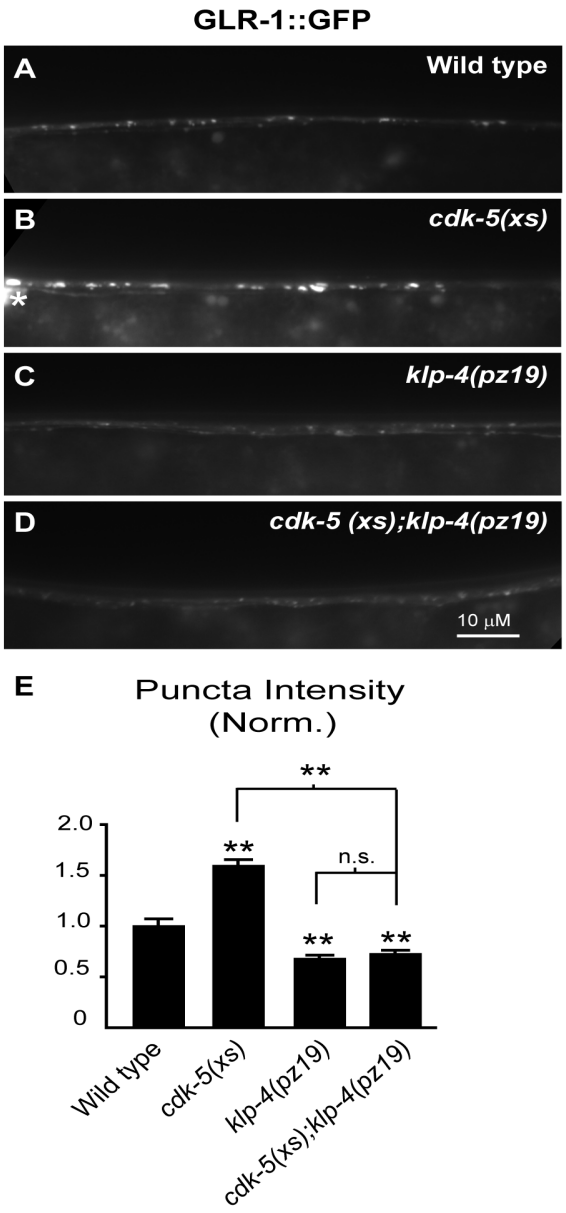

FIGURE S7. *klp-4(pz19)* mutation blocks the effects of *cdk-5* overexpression on GLR-1 in the VNC. (A-D) Representative images of GLR-1::GFP (*nuIs24*) in the anterior VNC of L4 wild type (A), wild type animals overexpressing *cdk-5* under the control of the *glr-1* promoter [*cdk-5(xs)*] (*pzIs2*) (B), *klp-4(pz19*) mutants (C) and *klp-4(pz19)* mutants overexpressing *cdk-5* [*cdk-5(xs)*] (D). The white asterisk marks a neuronal cell body. (E) Quantification of GLR-1::GFP puncta intensities (normalized) for the strains pictured in A-D. Mean and SEM are shown for *n* = 23 wild type, *n* = 23 *cdk-5(xs)*, *n* = 23 *klp-4* and *n* = 26 *cdk-5(xs);klp-4* animals. Values that differ significantly from wild type are indicated by asterisks above each bar, whereas other comparisons are marked by brackets (**$p \leq 0.001$, Tukey-Kramer test). n.s. denotes no significant difference between the indicated strains ($p>0.05$).